CAT-SAC: SOFT ACTOR-CRITIC WITH CURIOSITY-AWARE ENTROPY TEMPERATURE

Anonymous authors
Paper under double-blind review

ABSTRACT

The trade-off between exploration and exploitation has long been a crucial issue in reinforcement learning (RL). Most of the existing RL methods handle this problem by adding action noise to the policies, such as the Soft Actor-Critic (SAC) (Haarnoja et al., 2018a;b) that introduces an entropy temperature for maximizing both the external value and the entropy of the policy. However, this temperature is applied indiscriminately to all different environment states, undermining the potential of exploration. In this paper, we argue that the agent should explore more in an unfamiliar state, while less in a familiar state, so as to understand the environment more efficiently. To this purpose, we propose **C**uriosity-**A**ware entropy **T**emperature for SAC (CAT-SAC), which utilizes the curiosity mechanism in developing an instance-level entropy temperature. CAT-SAC uses the state prediction error to model curiosity because an unfamiliar state generally has a large prediction error. The curiosity is added to the target entropy to increase the entropy temperature for unfamiliar states and decrease the target entropy for familiar states. By tuning the entropy specifically and adaptively, CAT-SAC is encouraged to explore when its curiosity is large, otherwise, it is encouraged to exploit. Experimental results on the difficult MuJoCo benchmark testify that the proposed CAT-SAC significantly improves the sample efficiency, outperforming the advanced model-based / model-free RL baselines.

1 INTRODUCTION

Deep reinforcement learning (RL), with high-capacity deep neural networks (DNNs), has been applied to solve various complex decision-making problems, including video games (Mnih et al., 2015; Vinyals et al., 2019), chess games (Silver et al., 2017; 2018) as well as robotic manipulation (Kalashnikov et al., 2018). However, it is notorious for its high sample inefficiency (Kaiser et al., 2019). Even when solving a simple task, RL needs substantial interaction data to improve the policy. One of the major obstacles for achieving sample-efficiency is the difficulty of balancing exploration and exploitation. The RL agent needs to explore the environment to collect useful information as well as exploit the acquired knowledge to improve its policy. Most of the existing works either use intrinsic rewards (e.g., count-based bonuses (Bellemare et al., 2016) and state prediction error (Pathak et al., 2017; Burda et al., 2018b)) to strengthen exploration, or augment the action value with the entropy to control the proportion of exploration dynamically (Haarnoja et al., 2017; Ziebart et al., 2008). Among these approaches, Soft Actor-Critic (SAC) (Haarnoja et al., 2018a;b) achieves the superior performance on MuJoCo (Todorov et al., 2012), an OpenAI gym (Brockman et al., 2016) benchmark with complex continuous control tasks.

Specifically, SAC aims to maximize expected value while also maximizing the entropy:

$$\pi^* = \underset{\pi}{\operatorname{argmax}} \sum_{t=0}^{\infty} \mathbb{E}_{s_t, a_t \sim \rho_\pi}[r_t + \alpha \mathcal{H}(\pi(\cdot|s_t))], \tag{1}$$

where r_t is the environment reward at timestep t, s_t is the state, a_t is the action, ρ_π is the distribution of trajectory w.r.t. policy π, $\mathcal{H}$ is the entropy of the policy and α is the entropy temperature that weights the importance of the entropy term versus the external reward. The entropy temperature is critical in SAC since different values determine diverse patterns of agent behavior. Small α may lead the agent to over-optimize the state-action value and develop a greedy policy. Due to the lack of

exploration, the agent with a small α is likely to get stuck in a local optimal. On the other hand, over-optimize the entropy with large α causes the agent to act nearly uniformly and therefore hampers the ability to exploit the environment. To choose a reasonable temperature automatically, Haarnoja et al. (2018b) introduce a target entropy term and extends SAC to a constrained optimization problem, which performs empirically well on MuJoCo tasks (Brockman et al., 2016).

However, the target entropy is applied to all transitions equally during training, which neglects the particularity of different states – some states require less exploration while others need more (Tokic, 2010). The particularity of different states for exploration has been discovered for a long time. One of the important particularity is the internal curiosity w.r.t. the environment states. Intuitively, when playing a new game, humans make many different attempts at the beginning, and after they understand the basic logic of the game, they will not spend extra time trying the things they already know. This implies that a better exploration strategy is to explore when the agent is in unfamiliar states and exploit when it is in the familiar states. Therefore, optimizing the policy with a global target entropy without considering the particularity of different states may instead hamper the exploration of the agent. Researchers use internal curiosity as an auxiliary reward to encourage the exploration of the agent (Bellemare et al., 2016; Tang et al., 2017; Ostrovski et al., 2017). Among these methods, Burda et al. (2018b) propose Random Network Distillation (RND) (Burda et al., 2018b) to remedy the 'noisy TV' problem (Pathak et al., 2017)[1], which predicts the output of a fixed random network and demonstrates the excellent exploration ability on games with image input. Although Haarnoja et al. (2018b) have also considered the association between the curiosity and the entropy, they do not apply any relevant guidance to their proposed strategy of automatically tuning entropy temperature.

In order to dynamically adjust the exploration-exploitation strategy regarding the curiosity about states, we make the first attempt to introduce the curiosity to the target entropy term of SAC so that SAC can actively enlarge its entropy at unfamiliar states while reducing its entropy at familiar states. We named our method as CAT-SAC – SAC with **C**uriosity-**A**ware entropy **T**emperature, by seamlessly introducing the curiosity to augment the target entropy term. Specifically, CAT-SAC first augments the target entropy term by adding the zero mean curiosity. By this means, the agent is encouraged to explore more in an unfamiliar state as its target entropy is large (with positive curiosity) and to explore less at a familiar state as its target entropy is small (with negative curiosity). Then, CAT-SAC adopts an instance-level entropy temperature $\alpha(\mathrm{state})$ to replace the original global entropy temperature so as to learn different entropy temperatures for different states. The instance-level entropy temperature is curiosity-aware as it is supervised by the curiosity augmented target entropy. As for the curiosity model, current advanced methods e.g. RND (Burda et al., 2018b) may fail to model the curiosity for feature input (e.g., position, velocity). One of the major reasons is that different states with dramatic visual difference may have a little difference in feature so that RND has difficulty in distinguishing different state with feature inputs and fails to model the curiosity. To cope with this problem, we propose a novel curiosity model X-RND, which first synthesizes 'unvisited' feature states from the collected data by blending two visited states with random weight entry by entry. With the visited and the 'unvisited' states, X-RND learns to separate the 'unvisited' from the visited by contrastive self-supervised learning (He et al., 2020). By doing so, X-RND successfully prevents the curiosity about the 'unvisited' states from the influence of the visited states.

In summary, the main contributions of this paper are as follows: We propose a novel CAT-SAC model, which enables the agent to better trade-off the exploration versus exploitation according to different curiosity about states; To model curiosity for feature inputs, we propose a new curiosity model, X-RND, optimized by contrastive self-supervised learning. Experimental results testify that the proposed method significantly improves the sample-efficiency on complex and difficult continuous control tasks of the MuJoCo benchmark against the state-of-art model-based / model-free methods.

2 Related Work

Exploration is an essential issue for effective reinforcement learning (Kakade & Langford, 2002), and the problem of exploration has been widely studied (Wunder et al., 2010; Haarnoja et al., 2018a; Pathak et al., 2017; Lee et al., 2020; Zhang et al., 2020; Sekar et al., 2020; Stadie et al., 2018). The

[1] When predicting the dynamics, the curiosity model is prone to produce a large error w.r.t noisy observation, resulting in a large curiosity.

main researches on exploration include noise-based exploration (Wunder et al., 2010; Tokic, 2010; Mnih et al., 2015; Lillicrap et al., 2015), maximum entropy of policy exploration (Haarnoja et al., 2017; 2018a) and intrinsic bonus exploration (Pathak et al., 2017; Burda et al., 2018a; Achiam & Sastry, 2017; Burda et al., 2018b). Noise based exploration aims to balance the ratio of exploration/exploitation by introducing a random policy noise. The most relevant to CAT-SAC is the maximum entropy exploration and the intrinsic bonus.

Maximum Entropy RL. Maximum entropy RL optimizes policies by maximizing the expected return and the expected entropy of the policy simultaneously (Haarnoja et al., 2017) (Haarnoja et al., 2018a). This framework has been used in many fields, such as reverse reinforcement learning (Ziebart et al., 2008) and optimal control (Roy et al., 2013). Recently, the maximum entropy framework has been successfully incorporated into Q-learning and policy gradient methods to improve sample efficiency, such as soft Q-learning algorithm (Haarnoja et al., 2017) and soft actor-critic (SAC) algorithm (Haarnoja et al., 2018a; 2019).

Soft Q-learning learns stochastic energy-based policies with approximate inference via stein variational gradient descent (SVGD) (Liu & Wang, 2016). However, approximate inference procedures become complex in continuous action spaces. Haarnoja et al. (2018a) present a convergence proof for policy iteration in the maximum entropy framework, known as soft actor-critic (SAC), which avoids the complexity and potential instability associated with the approximate inference of soft Q-learning. Haarnoja et al. (2019) further propose an extension to the soft actor-critic algorithm that the temperature parameter can be optimized adaptively. While SAC provides for both sample efficient learning and stability in continuous control tasks, the temperature is applied indiscriminately to all different states. This will result in some useless exploration and undermining the potential of exploration. The proposed algorithm is based on the framework of SAC. Our goal is to develop a curiosity-aware entropy temperature so that agents can have different trade-offs between exploration and exploitation at different scenarios.

Intrinsic Bonus. Intrinsic bonus exploration methods encourage the agent to explore by introducing an intrinsic bonus as an auxiliary reward. One of the common intrinsic bonuses is defined based on visit-count that indicates how many times the agent performed action a at state s (Bellemare et al., 2016; Tang et al., 2017; Ostrovski et al., 2017; Fox et al., 2018). Another class of intrinsic bonus is calculated according to errors of predicting dynamics (Pathak et al., 2017; Burda et al., 2018a; Achiam & Sastry, 2017). They first learn forward dynamics to predict the next observation given the current observation and agent's action. The prediction error represents the agent's familiarity about the state. These approaches focus on maximizing the prediction error as an intrinsic reinforcement learning objective. However, maximizing such prediction errors of forwarding dynamics will tend to cause the agent to be attracted to stochastic transitions (Burda et al., 2018b), e.g., the "noisy TV". Burda et al. (2018b) propose random network distillation (RND) bonus to handle this undesirable stochasticity. RND predicts the output of a fixed randomly initialized neural network based on the current observation. Therefore, the predicted output is deterministic. Different from RND, our proposed curiosity model is able to handle feature input by optimizing with the contrastive self-supervised loss (He et al., 2020).

3 PRELIMINARIES

In this section, we introduce the background and annotations of reinforcement learning and the two key ingredients of our method, i.e., SAC (Haarnoja et al., 2018a;b) and RND (Burda et al., 2018b).

3.1 REINFORCEMENT LEARNING

We consider a standard RL framework where an agent interacts with an environment according to the observation in discrete time. Formally, the agent observes a state s_t (e.g., position, velocity) from the environment at each time step t and then chooses an action a_t according to its policy π. The environment returns a reward r_t and the next state $s_{t+1} \sim p_e(s_t, a_t)$, where p_e is the environment transition mapping. The return of a trajectory from timestep t is $\eta_t = \sum_{k=0}^{\infty} \gamma^k r_{t+k}$, where $y \in [0, 1)$ is the discount factor. RL aims to optimize the policy to maximize the expected return from each state s_t.

3.2 SOFT ACTOR-CRITIC

SAC (Haarnoja et al., 2018a) is an off-policy actor-critic method based on the maximum entropy RL framework (Ziebart et al., 2008), which aims to maximize both the return and the policy entropy, as described in Equ. (1). It uses a neural network with parameter θ for Q-value Q_θ, and uses anther neural network parameterized by ϕ for the policy π_ϕ. To update these parameters, SAC alternates between a soft policy evaluation and a soft policy improvement. At the soft policy evaluation step, θ is updated by minimizing the following cost function:

$$\mathcal{L}_{\text{critic}}(\theta) = \mathbb{E}_{s_t,a_t\sim\mathcal{D}}[||Q_\theta(s_t,a_t) - Q^{\text{target}}(s_t,a_t)||_2^2], \tag{2}$$

$$\text{where } Q^{\text{target}}(s_t,a_t) = r_t + \gamma\mathbb{E}_{s_{t+1}\sim p_e, a_{t+1}\sim\pi_\phi}[\hat{Q}(s_{t+1},a_{t+1}) - \alpha log(\pi_\phi(a_{t+1}|s_{t+1}))], \tag{3}$$

where $\mathcal{D}$ is an experience replay buffer, α is the entropy temperature, and $\hat{Q}$ is the target Q function whose parameters are periodically updated from the learned Q_θ. At the soft policy improvement step, the policy π with its parameters ϕ is updated by minimizing the following objective:

$$\mathcal{L}_{\text{actor}}(\phi) = \mathbb{E}_{s_t\sim\mathcal{D},a_t\sim\pi_\phi}[\alpha log\pi_\phi(a_t|s_t) - Q_\theta(s_t,a_t)]. \tag{4}$$

Here, the policy models a Gaussian with mean and variance to handle continuous control problems. In order to automatically tune α, Haarnoja et al. (2018b) introduces a constraint target entropy $\tilde{\mathcal{H}}$, so that α is learned to meet the constraints during the whole training process:

$$\mathcal{L}(\alpha) = \mathbb{E}_{s_t\sim\mathcal{D},a_t\sim\pi_\phi}[-\alpha log\pi(a_t|s_t) - \alpha\tilde{\mathcal{H}}]. \tag{5}$$

3.3 RANDOM DISTILLATION NETWORK

Random Network Distillation (RND) (Burda et al., 2018b), a prediction-based method for encouraging exploration through curiosity, which manages to exceed average human performance on Montezuma's Revenge (Badia et al., 2020). The RND exploration bonus is defined as the state prediction error of a neural $f_\omega(s_t)$ predicting features of the state given by a fixed randomly initialized neural network $\hat{f}(s_t)$. The exploration bonus and the loss function are:

$$c_\omega(s_t) = ||f_\omega(s_t) - \hat{f}(s_t)||_2^2 \text{ and } \mathcal{L}(\omega) = \mathbb{E}_{s_t\sim\mathcal{D}}[c_\omega(s_t)]. \tag{6}$$

In unfamiliar states, it's hard for f_ω to predict the output of $\hat{f}$, and hence the prediction error $c(s_t)$ is high. By measuring how hard it is to predict the output of $\hat{f}$ on these states, RND incentivizes visiting unfamiliar states.

4 CAT-SAC

In this section, we present CAT-SAC : **C**uriosity-**A**ware entropy **T**emperature for Soft Actor-Critic. In the design of CAT-SAC, we integrate three key ingredients, i.e., the curiosity augmented target entropy, the instance-level entropy temperature, and the curiosity model X-RND for feature input, into a single framework.

4.1 CURIOSITY AUGMENTED TARGET ENTROPY

Haarnoja et al. (2018b) reformulates SAC from the maximum entropy RL framework to a constraint satisfaction problem by introducing the target entropy to tune the entropy temperature automatically. However, applying the target entropy to all transitions neglects the particularity of different states, i.e., an unfamiliar state often requires more exploration. To enable the agent to increase the entropy when it's in an unfamiliar state, we inject the curiosity to the target entropy. Specifically, we first normalize the curiosity $c(s)$ w.r.t state s, and then add it to the original target entropy $\tilde{\mathcal{H}}$:

$$h(s) = \tilde{\mathcal{H}} + \frac{c(s) - \mu}{\sigma}, \tag{7}$$

where μ and σ are the running mean and running standard deviation of $c(s)$ respectively. From the Equ.(7), the expectation of the proposed curiosity augmented target entropy is $\mathbb{E}_s[h(s)] = \tilde{\mathcal{H}}$, therefore the new target entropy is consistent with the original one in expectation. In this manner, the target entropy in an unfamiliar state is pushed above the expectation and thus the agent is encouraged to explore more in that state; on the contrary, the target entropy in the familiar state is pressed down to regulate the behavior of the agent to exploit efficiently.

4.2 INSTANCE-LEVEL ENTROPY TEMPERATURE

The entropy temperature is the most crucial component in either SAC or CAT-SAC, as it is the bridge connecting the target entropy and the policy. Therefore, to really cast different target entropy to the policy at different states, we need to turn the original global entropy temperature α into an instance-level entropy temperature $\alpha_\delta(s)$, whose target is:

$$\delta^* = \underset{\delta}{\operatorname{argmin}}\, \mathbb{E}_{s_t \sim \mathcal{D}, a_t \sim \pi_\phi}[-\alpha_\delta(s_t) log \pi_\phi(a_t|s_t) - \alpha_\delta(s_t) h(s_t)]. \tag{8}$$

From Equ.(8), we can observe that if α is state-independent, then the expectation term in Equ.(8) will be equivalent to the original of Equ.(5), therefore, the effect of the curiosity augmented target entropy will not be reflected in the policy.

Since the instance-level entropy temperature may weaken the connection across states in Equ. (8), $\alpha_\delta(s_t)$ is likely to trivially enforcing $\log \pi(a_t|s_t)$ to approach $h(s_t)$ under the context of state s_t. As mentioned by Haarnoja et al. (2018b), forcing the entropy to be a target entropy will hamper the flexibility of the policy. To prevent the $\alpha_\delta(s_t)$ from doing so, instead of s_t, we use the curiosity $c(s_t)$ as the context of the entropy temperature, which projects different states to compact values so as to cluster those states with the same level of unfamiliarity to share the same entropy temperature:

$$\alpha_\delta(s_t) = g_\delta(c(s_t)), \tag{9}$$

where g_δ a linear layer with parameter δ. More details about the g_δ is presented in Appendix. To further reduce the space of the entropy temperature, we further project $c(s_t)$ into its closest integer. One can treat our method as a stratified SAC regarding different discrete curiosity levels.

4.3 X-RND BASED ON SELF-SUPERVISED CONTRASTIVE LEARNING

In our framework, the curiosity values of familiar states should be relatively smaller than those of unfamiliar states. Burda et al. (2018b) have demonstrated that RND works well in modeling curiosity for hard exploration tasks with image input. However, we found that RND works poorly with feature input. Especially for the features of unvisited states that are close to the visited states', RND is likely to produce low prediction errors. Therefore, the curiosity model based on state prediction error like RND, besides minimizing the prediction error Equ.(6) of the visited states, may need extra supervision to learn how to maintain the prediction error of the unvisited states to a certain extent. To this end, we develop X-RND, which includes an additional contrastive loss (He et al., 2020; Schmidhuber, 2015) to push the curiosity values of potential unseen states s' above a margin value. The loss function of X-RND is formulated as:

$$\mathcal{L}(\omega) = \mathbb{E}_{s_t \sim \mathcal{D}}\big[c_\omega(s) + \beta \max(m - c_\omega(s'), 0)\big], \tag{10}$$

where m is the curiosity margin for unvisited states and β is the hyperparameter that weighs the importance of the contrastive loss term. In order to obtain the unvisited states s', X-RND constructs the potential unvisited states from the visited states. Specifically, X-RND randomly samples a set of states from the replay buffer, and then randomly fuses any two different states with different weights. Formally, $s' = s_1 + \epsilon \times (s_2 - s_1)$, where $s_1, s_2 \sim \mathcal{D}$, $s_1 \neq s_2$ and $\epsilon \sim \mathcal{U}[0, 1.5]^{|s|}$. $|s|$ is the dimension of state feature and $\mathcal{U}[0, 1.5]^{|s|}$ is the $|s|$-dimensional uniform distribution with range [0, 1.5].[2] By doing so, the synthesized 'unvisited' states still obey the similar statistical characteristics as the visited states [3]. By pushing the prediction errors of these self-constructed states above the curiosity margin, X-RND significantly improves the performance of the curiosity model with feature inputs, as demonstrated in the next section.

5 EXPERIMENTS

We begin by demonstrating the effectiveness of the curiosity-aware exploration strategy on difficult continuous control OpenAI Gym environments (Brockman et al., 2016) in Sec. 5.1 against current

[2] With upper bound larger than 1, the value of the synthesized state can be beyond the range of the visited states.

[3] Although a few synthesized states possibly exist in the visited states, it would not have a great impact since the visited states are much more likely to be sampled during training so that their prediction error would be pulled back in expectation.

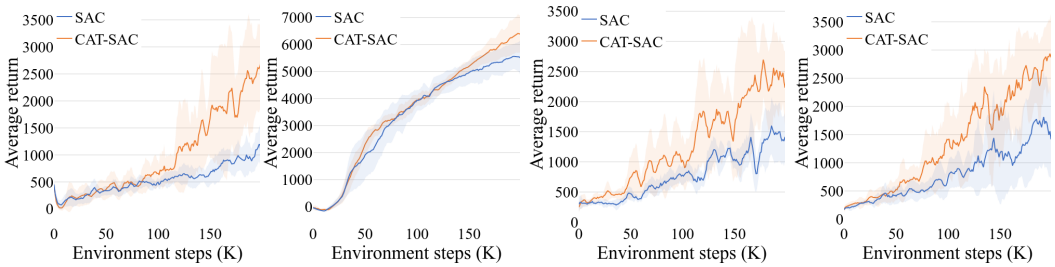

(a) Ant (b) Cheetah (c) Walker (d) Hopper

Figure 1: Evaluation curves of SAC (Haarnoja et al., 2018b) and CAT-SAC on (a) Ant, (b) Cheetah, (c) Walker, and (d) Hopper environments. The solid line and shaded regions represent the mean and the standard deviation across four runs, respectively.

Table 1: Performance on OpenAI Gym at 200K timesteps. The results show the mean and standard deviation across four runs. For baselines, we report the best number in SUNRISE (Lee et al., 2020). The best results are highlighted in bold.

	Cheetah	Walker	Hopper	Ant
METRPO (2018)	2283.7 $\pm$ 900.4	-1609.3 $\pm$ 657.5	1272.5 $\pm$ 500.9	282.2 $\pm$ 18
PETS (2018)	2288.4 $\pm$ 1019.0	282.5 $\pm$ 501.6	114.9 $\pm$ 621.0	1165.5 $\pm$ 226.9
POPLIN-A (2019)	1562.8 $\pm$ 1136.7	-105.0 $\pm$ 249.8	202.5 $\pm$ 962.5	1148.4 $\pm$ 438.3
POPLIN-P (2019)	4235.0 $\pm$ 1133.0	597.0 $\pm$ 478.8	2055.2 $\pm$ 613.8	2330.1 $\pm$ 320.9
TD3 (2018)	3015.7 $\pm$ 969.8	-516.4 $\pm$ 812.2	1816.6 $\pm$ 994.8	870.1 $\pm$ 283.8
SUNRISE (2020)	5370.6 $\pm$ 483.1	1926.2 $\pm$ 694.8	2601.9 $\pm$ 306.5	1627.0 $\pm$ 292.7
SAC (2018b)	5511.9 $\pm$ 616.1	1414.8 $\pm$ 400.7	1415.2 $\pm$ 692.1	1028.8 $\pm$ 321.7
CAT-SAC	**6380.4** $\pm$ **690.1**	**2231.0** $\pm$ **615.7**	**2869.4** $\pm$ **768.7**	**2725.9** $\pm$ **811.2**

advanced model-based / model-free baselines. To better understand the benefit of the proposed curiosity model for feature inputs, we design a minimal grid-world environment to provide a concise and straightforward comparison between X-RND and RND in Sec. 5.2. After that, we ablate different choices of the important components and hyperparameters of CAT-SAC in Sec. 5.3.

5.1 MuJoCo Results

CAT-SAC is evaluated on four continuous control tasks from OpenAI Gym (Brockman et al., 2016), i.e., Ant, Walker, Cheetah as well as Hopper. Following the same experiment settings of SUNRISE (Lee et al., 2020), we compare CAT-SAC with METRPO (Kurutach et al., 2018), a combination of TRPO (Schulman et al., 2015) and ensembles of dynamics models; PETS (Chua et al., 2018), an advanced model-based (MB) RL method based on ensembles of dynamics models; POPLIN-P (Wang & Ba, 2019), a state-of-the-art MBRL method; POPLIN-A (Wang & Ba, 2019), a variant of POPLIN-P by injecting noise to the action space. We also compare CAT-SAC with three state-of-the-art model-free RL methods, TD3 (Fujimoto et al., 2018), SAC (Haarnoja et al., 2018b) and SUNRISE (Lee et al., 2020). For our method, we consider a combination of SAC and CAT-SAC. The whole algorithm for CAT-SAC is described in Alg. 1 in the Appendix. Following the experiment setups in SUNRISE, the curves and results in our experiments are calculated after 200K timesteps. Each experiment is conducted four times with the mean and the standard deviation reported. More experimental details are presented in the Appendix.

As shown in Tab. 1, CAT-SAC outperforms all of the baselines on all tasks. As for the performance on Cheetah and Walker, CAT-SAC makes a breakthrough that exceeding 6000 and 2000 on average, respectively, within 200K environment frames. On tasks Ant and Hopper, we observe that the performance of SAC and CAT-SAC almost coincides at the early stage, however, CAT-SAC gets away from the flat slope quickly and improves faster, which implies CAT-SAC is more capable of exploiting acquired knowledge and execute an efficient exploration. In comparison with all base-

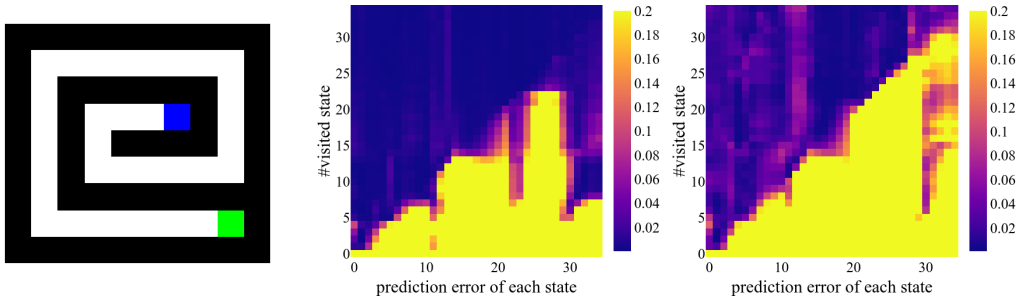

(a) Swiss Roll Maze (b) RND (c) X-RND

Figure 2: Demonstration on (a) the Swiss Roll maze environment, (b) prediction error of RND (c) prediction error of X-RND. The agent starts from the blue block and moves to the green block. (b)(c) shows the state prediction errors of all movable blocks (x-axis) given the number of visited blocks (y-axis) to the agent.

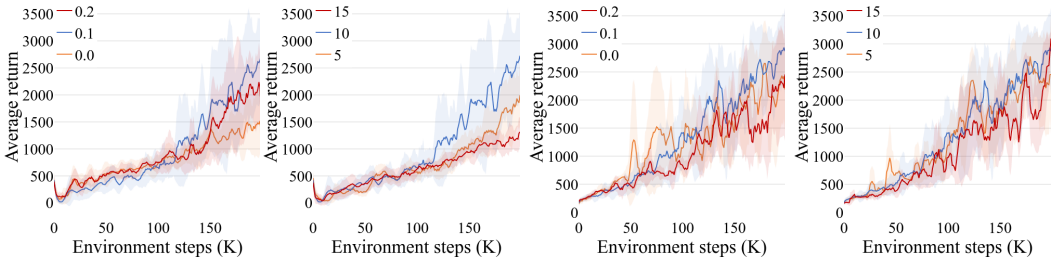

(a) Ant (β) (b) Ant (m) (c) Hopper (β) (d) Hopper (m)

Figure 3: Evaluation curves of CAT-SAC with different values of hyperparameters β and m. From left to right, there are figures for (a) β on Ant, (b) m on Ant, (c) β on Hopper and (d) m on Hopper. The solid line and shaded regions represent the mean and the standard deviation across four runs, respectively.

lines, CAT-SAC is more compute-efficient since it does not require any ensemble of dynamics and planning during the evaluation phase.

5.2 X-RND VERSUS RND WITH FEATURE INPUTS

We present a simple example to highlight the effectiveness and robustness of the proposed curiosity model X-RND for feature input. We introduce a grid-world environment, *Swiss Roll* maze, as depicted in Fig. 2a. The agent is moving from the blue block to the green block. Every time the agent arrives at a new block, both RND and X-RND train on features (i.e., position) of all visited blocks. Since we aim to analyze the problem of RND with feature inputs and the advantage of X-RND, we simply adopt the agent with the optimal policy for moving. We record the curiosity values of all movable blocks of both methods w.r.t. the amount of unique visited states and plots them in Fig. 2b and Fig. 2c, respectively. More experimental details on this toy settings are presented in the Appendix.

In Fig. 2b and Fig. 2c, values of each row present the curiosity values of all visited / unvisited. The curiosity values are clipped within the curiosity margin (m = 0.2 for this toy experiment). Ideally, values in the upper triangle of the figure should be closed to 0, while values in the lower triangle should be closed to the curiosity margin. From Fig. 2b and Fig. 2c, we can observe that, when the agent visits 10 unique states (index 10 at y-axis), RND has faultily regarded the distant and unvisited states (index from 30 to the last at x-axis) as visited states and produces low prediction errors for them; while X-RND successfully sustains the curiosity for these states. A more appealing property of X-RND is that X-RND is more like to form a sharp contrast between the explored and unexplored areas (with a clear diagonal). It is more important to have accurate curiosity prediction for the near unvisited states than keeping the curiosity about the very distant state high, since those near states

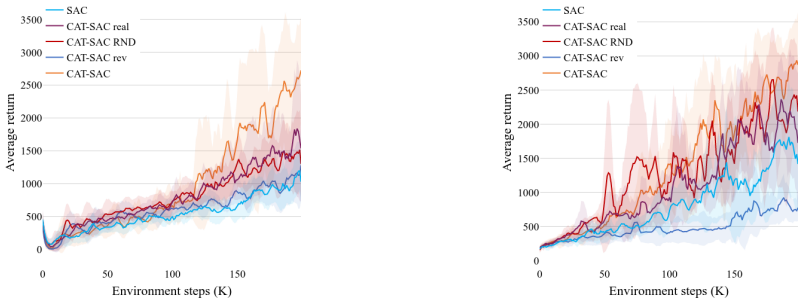

(a) Ant (b) Hopper

Figure 4: Evaluation curves for CAT-SAC on (a) Ant and (b) Hopper tasks. The solid line and shaded regions represent the mean and standard deviation, respectively, across four runs.

are more likely to be visited. This phenomenon implies the synthesized states are likely to fall in the border between the explored and unexplored. More visual comparison of RND and X-RND are presented in the Appendix.

5.3 Ablation Study

In this section, we ablate the effects of different values of the hyperparameters as well as different components of CAT-SAC on Ant and Hopper, which should be representative of all tasks.

Effects of different hyperparameters. We analyze the effects of different values of the hyperparameters CAT-SAC, i.e., the curiosity margin m and the importance weight β in Equ.(10). Notice that when β equals 0, the X-RND in SAC is the same as RND. As depicted in Fig. 3a and Fig. 3c, CAT-SAC with positive β achieves better performance on both tasks, which means that a better curiosity model X-RND indeed help improve the performance of CAT-SAC. However, we also observe that the larger β is not necessary to bring more improvement. We suppose the reason is that a large importance weight on the contrastive loss may cause the RND loss for familiar states difficult to decrease. As for the choice of the curiosity margin m, we found that CAT-SAC is more sensitive to different values of m on task Ant (Fig. 3b). The reason might also is that m determines the range of the curiosity and therefore influence the distribution of $c(s)$, which is the critical component in CAT-SAC. But overall, with different values of β and m, CAT-SAC still outperforms SAC, which implies that our method consistently gains improvement.

Individual effect of each component. In our full CAT-SAC, curiosity from X-RND is discretized into integer and normalized to have zero mean, and then added to the original target entropy. To evaluate the effect of each component, we conduct experiment on i) *real*, which does not discretize the curioisty 4.2; ii) *RND*, which use RND to predict curiosity; (iii) *rev*, which subtracts the curiosity from the target effect. Among these settings, only *rev* is contrary to our motivation, that's, the agent should explore more in unfamiliar states. Fig. 4 shows the performance of CAT-SAC under different settings. From the results, we observe that turning off any component would decrease the performance of the full version. And except for *rev*, CAT-SAC with different component turning off still outperforms the baselines with a sharp margin. It implies that our motivation actually helpful in developing a better exploration-exploitation trade-off strategy. By utilizing all the proposed techniques, we obtain the best performance in all environments. From this comparison, we see that all proposed components have a positive effect on improving the sample-efficiency of CAT-SAC.

6 Conclusion

In this paper, we present CAT-SAC, a simple framework unified curiosity and entropy maximization RL. In particular, CAT-SAC encourages a large entropy in unfamiliar states and a small entropy in familiar states for a better trade-off between exploration and exploitation. To model curiosity for feature input, we also propose a new prediction-based model, X-RND. Our experiments show that the full CAT-SAC consistently improves the performances of SAC and outperforms state-of-the-art RL algorithms in complex control tasks.

REFERENCES

Joshua Achiam and Shankar Sastry. Surprise-based intrinsic motivation for deep reinforcement learning. *arXiv preprint arXiv:1703.01732*, 2017.

Adrià Puigdomènech Badia, Bilal Piot, Steven Kapturowski, Pablo Sprechmann, Alex Vitvitskyi, Daniel Guo, and Charles Blundell. Agent57: Outperforming the atari human benchmark. *arXiv preprint arXiv:2003.13350*, 2020.

Marc Bellemare, Sriram Srinivasan, Georg Ostrovski, Tom Schaul, David Saxton, and Remi Munos. Unifying count-based exploration and intrinsic motivation. In *Advances in neural information processing systems*, pp. 1471–1479, 2016.

Greg Brockman, Vicki Cheung, Ludwig Pettersson, Jonas Schneider, John Schulman, Jie Tang, and Wojciech Zaremba. Openai gym. *arXiv preprint arXiv:1606.01540*, 2016.

Yuri Burda, Harri Edwards, Deepak Pathak, Amos Storkey, Trevor Darrell, and Alexei A Efros. Large-scale study of curiosity-driven learning. In *International Conference on Learning Representations*, 2018a.

Yuri Burda, Harrison Edwards, Amos Storkey, and Oleg Klimov. Exploration by random network distillation. In *International Conference on Learning Representations*, 2018b.

Kurtland Chua, Roberto Calandra, Rowan McAllister, and Sergey Levine. Deep reinforcement learning in a handful of trials using probabilistic dynamics models. In *Advances in Neural Information Processing Systems*, pp. 4754–4765, 2018.

Lior Fox, Leshem Choshen, and Yonatan Loewenstein. Dora the explorer: Directed outreaching reinforcement action-selection. In *International Conference on Learning Representations*, 2018.

Scott Fujimoto, Herke Van Hoof, and David Meger. Addressing function approximation error in actor-critic methods. *arXiv preprint arXiv:1802.09477*, 2018.

Tuomas Haarnoja, Haoran Tang, Pieter Abbeel, and Sergey Levine. Reinforcement learning with deep energy-based policies. *arXiv preprint arXiv:1702.08165*, 2017.

Tuomas Haarnoja, Aurick Zhou, Pieter Abbeel, and Sergey Levine. Soft actor-critic: Off-policy maximum entropy deep reinforcement learning with a stochastic actor. In *International Conference on Machine Learning*, pp. 1861–1870, 2018a.

Tuomas Haarnoja, Aurick Zhou, Kristian Hartikainen, George Tucker, Sehoon Ha, Jie Tan, Vikash Kumar, Henry Zhu, Abhishek Gupta, Pieter Abbeel, et al. Soft actor-critic algorithms and applications. *arXiv preprint arXiv:1812.05905*, 2018b.

Tuomas Haarnoja, Sehoon Ha, Aurick Zhou, Jie Tan, George Tucker, and Sergey Levine. Learning to walk via deep reinforcement learning. In *Proceedings of Robotics: Science and Systems*, FreiburgimBreisgau, Germany, June 2019. doi: 10.15607/RSS.2019.XV.011.

Kaiming He, Haoqi Fan, Yuxin Wu, Saining Xie, and Ross Girshick. Momentum contrast for unsupervised visual representation learning. In *Proceedings of the IEEE/CVF Conference on Computer Vision and Pattern Recognition*, pp. 9729–9738, 2020.

Lukasz Kaiser, Mohammad Babaeizadeh, Piotr Milos, Blazej Osinski, Roy H Campbell, Konrad Czechowski, Dumitru Erhan, Chelsea Finn, Piotr Kozakowski, Sergey Levine, et al. Model-based reinforcement learning for atari. *arXiv preprint arXiv:1903.00374*, 2019.

Sham Kakade and John Langford. Approximately optimal approximate reinforcement learning. In *ICML*, volume 2, pp. 267–274, 2002.

Dmitry Kalashnikov, Alex Irpan, Peter Pastor, Julian Ibarz, Alexander Herzog, Eric Jang, Deirdre Quillen, Ethan Holly, Mrinal Kalakrishnan, Vincent Vanhoucke, et al. Qt-opt: Scalable deep reinforcement learning for vision-based robotic manipulation. *arXiv preprint arXiv:1806.10293*, 2018.

Thanard Kurutach, Ignasi Clavera, Yan Duan, Aviv Tamar, and Pieter Abbeel. Model-ensemble trust-region policy optimization. *arXiv preprint arXiv:1802.10592*, 2018.

Kimin Lee, Michael Laskin, Aravind Srinivas, and Pieter Abbeel. Sunrise: A simple unified framework for ensemble learning in deep reinforcement learning. *arXiv preprint arXiv:2007.04938*, 2020.

Timothy P Lillicrap, Jonathan J Hunt, Alexander Pritzel, Nicolas Heess, Tom Erez, Yuval Tassa, David Silver, and Daan Wierstra. Continuous control with deep reinforcement learning. *arXiv preprint arXiv:1509.02971*, 2015.

Qiang Liu and Dilin Wang. Stein variational gradient descent: A general purpose bayesian inference algorithm. In *Advances in neural information processing systems*, pp. 2378–2386, 2016.

Volodymyr Mnih, Koray Kavukcuoglu, David Silver, Andrei A Rusu, Joel Veness, Marc G Bellemare, Alex Graves, Martin Riedmiller, Andreas K Fidjeland, Georg Ostrovski, et al. Human-level control through deep reinforcement learning. *nature*, 518(7540):529–533, 2015.

Georg Ostrovski, Marc G Bellemare, Aäron Oord, and Rémi Munos. Count-based exploration with neural density models. In *International Conference on Machine Learning*, pp. 2721–2730, 2017.

Deepak Pathak, Pulkit Agrawal, Alexei A Efros, and Trevor Darrell. Curiosity-driven exploration by self-supervised prediction. In *Proceedings of the IEEE Conference on Computer Vision and Pattern Recognition Workshops*, pp. 16–17, 2017.

Nicholas Roy, Paul Newman, and Siddhartha Srinivasa. On stochastic optimal control and reinforcement learning by approximate inference. 2013.

Jürgen Schmidhuber. Deep learning in neural networks: An overview. *Neural networks*, 61:85–117, 2015.

John Schulman, Sergey Levine, Pieter Abbeel, Michael Jordan, and Philipp Moritz. Trust region policy optimization. In *International conference on machine learning*, pp. 1889–1897, 2015.

Ramanan Sekar, Oleh Rybkin, Kostas Daniilidis, Pieter Abbeel, Danijar Hafner, and Deepak Pathak. Planning to explore via self-supervised world models. *arXiv preprint arXiv:2005.05960*, 2020.

David Silver, Julian Schrittwieser, Karen Simonyan, Ioannis Antonoglou, Aja Huang, Arthur Guez, Thomas Hubert, Lucas Baker, Matthew Lai, Adrian Bolton, et al. Mastering the game of go without human knowledge. *nature*, 550(7676):354–359, 2017.

David Silver, Thomas Hubert, Julian Schrittwieser, Ioannis Antonoglou, Matthew Lai, Arthur Guez, Marc Lanctot, Laurent Sifre, Dharshan Kumaran, Thore Graepel, et al. A general reinforcement learning algorithm that masters chess, shogi, and go through self-play. *Science*, 362(6419):1140–1144, 2018.

Bradly C Stadie, Ge Yang, Rein Houthooft, Xi Chen, Yan Duan, Yuhuai Wu, Pieter Abbeel, and Ilya Sutskever. Some considerations on learning to explore via meta-reinforcement learning. *arXiv preprint arXiv:1803.01118*, 2018.

Haoran Tang, Rein Houthooft, Davis Foote, Adam Stooke, OpenAI Xi Chen, Yan Duan, John Schulman, Filip DeTurck, and Pieter Abbeel. # exploration: A study of count-based exploration for deep reinforcement learning. In *Advances in neural information processing systems*, pp. 2753–2762, 2017.

Emanuel Todorov, Tom Erez, and Yuval Tassa. Mujoco: A physics engine for model-based control. In *2012 IEEE/RSJ International Conference on Intelligent Robots and Systems*, pp. 5026–5033. IEEE, 2012.

Michel Tokic. Adaptive ε-greedy exploration in reinforcement learning based on value differences. In *Annual Conference on Artificial Intelligence*, pp. 203–210. Springer, 2010.

Oriol Vinyals, Igor Babuschkin, Wojciech M Czarnecki, Michaël Mathieu, Andrew Dudzik, Junyoung Chung, David H Choi, Richard Powell, Timo Ewalds, Petko Georgiev, et al. Grandmaster level in starcraft ii using multi-agent reinforcement learning. *Nature*, 575(7782):350–354, 2019.

Tingwu Wang and Jimmy Ba. Exploring model-based planning with policy networks. *arXiv preprint arXiv:1906.08649*, 2019.

Michael Wunder, Michael L Littman, and Monica Babes. Classes of multiagent q-learning dynamics with epsilon-greedy exploration. In *Proceedings of the 27th International Conference on Machine Learning (ICML-10)*, pp. 1167–1174. Citeseer, 2010.

Yunzhi Zhang, Pieter Abbeel, and Lerrel Pinto. Automatic curriculum learning through value disagreement. *arXiv preprint arXiv:2006.09641*, 2020.

Brian D Ziebart, Andrew L Maas, J Andrew Bagnell, and Anind K Dey. Maximum entropy inverse reinforcement learning. In *Aaai*, volume 8, pp. 1433–1438. Chicago, IL, USA, 2008.

A CAT-SAC: EXPERIMENTAL SETUPS

Environments. We evaluate the performance of CAT-SAC on four complex environments from OpenAI Gym (Brockman et al., 2016), i.e., Ant, Cheetah, Walker, and Hopper. Observation in these tasks is in the form of features.

Training details. We consider a combination of SAC and CAT-SAC using the publicly released implementation repository (https://github.com/thu-ml/tianshou) with slight modifications on hyperparameters and architectures in order to match the implementation of RLKit (https://github.com/vitchyr/rlkit). The complete algorithm is depicted in Alg. 1. The detailed hyperparameters used in CAT-SAC is presented in Tab. 2

Details of the instance-level entropy temperature. In order to automatically tune the entropy temperature in a similar way to (Haarnoja et al., 2018b), we do not adopt deep neural networks for the instance-level entropy temperature. Instead, we initialize a list of scalar variables. Each variable is assigned to a integer index, ranging from $-|\text{target entropy}|$ to $|\text{target entropy}|$. Given the discrete curiosity input, we match it with the variable with the closest index, and then the same optimization process in (Haarnoja et al., 2018b) is conducted to optimize these variables. As for the input under the *real* setting in Sec. 5.3, we match it with the two variables with the closest indexes and calculate the weights of these variables so that the sum of the weighted indexes assembles the curiosity value. Then the sum of the weighted variables is treated as the entropy temperature.

Algorithm 1 Soft Actor-Critic with Curiosity-Aware Entropy Temperature

Input: initial policy parameters ϕ, Q-function parameters θ_1, θ_2, empty replay buffer $\mathcal{D}$
Set target parameters equal to main parameters $\theta_{\text{targ},1} \leftarrow \theta_1$, $\theta_{\text{targ},2} \leftarrow \theta_2$
repeat
  Observe state s_t and select action $a_t \sim \pi_\phi(\cdot|s_t)$
  Execute a_t in the environment
  Observe next state s_{t+1}, reward r_t, and done signal d_t to indicate whether s_{t+1} is terminal
  Store $(s_t, a_t, r_t, s_{t+1}, d_t)$ in replay buffer $\mathcal{D}$
  if d_t is true **then**
    Reset environment state.
    Sample set of states $\{s\}$ from $\mathcal{D}$ and sythesize a new set of states $\{s'\}$
    Update f_ω by optimizing Equ.(10)
    Calculate the new mean μ and standard deviation σ of $\{c(s)\}$
  end if
  if it's time to update **then**
    Randomly sample a batch of transitions, $B = \{(s_t, a_t, r_t, s_{t+1}, d)\}$ from $\mathcal{D}$
    Calculate $c(s_t)$ and $\alpha_\delta(s_t)$ for the rest optimizations
    Update Q-functions by one step of gradient descent using $\nabla_{\theta_i} \frac{1}{|B|} \mathcal{L}_{\text{critic}}(\theta_i)$ for i=1,2
    Update policy by one step of gradient ascent using $\nabla_\phi \frac{1}{|B|} \sum_{s \in B} \mathcal{L}_{\text{actor}}(\phi)$
    Update target networks with $\theta_{\text{targ},i} \leftarrow \rho\theta_{\text{targ},i} + (1-\rho)\theta_i$ for i=1,2
    Construct curiosity augmented target entropy $h(s_t)$ by Equ.(7)
    Update α_δ by one step of gradient descent using $\nabla_\delta \frac{1}{|B|} \mathcal{L}(\delta)$
  end if
until convergence

Table 2: Values of hyperparameters used in this paper.

Hyperparameter	Value	Hyperparameter	Value
#training frames	2e7	#frames between evaluations	1e3
Backbone	MLP	Non-linearity	ReLU
Backbone (g)	Vector	(X-)RND feature size	128
Hidden layers	2	Optimizer	Adam
Hidden layers ((X-)RND f)	4	Critic target update freq	1
Hidden units	256	Learning rate	3e-4
Batch size	256	Discount γ	0.99
Initial temperature	1	Curioisty margin m	10
#batch for update (X-)RND	100	Importance weight β	0.1
Polyak factor τ	0.005	Target entropy	$-\lvert$ action space $\rvert$
Replay buffer size	1e6	Evaluation episodes	10
Hidden layer (toy)	1	Hidden units (toy)	16
Importance weight β (toy)	0.5	(X-)RND feature size (toy)	16
Curiosity margin m (toy)	0.2	Batch size (toy)	64

B SWISS ROLL MAZE: EXPERIMENTAL SETUPS

Environment. As depicted in Sec. 5.2. In this environment, only position features are provided.

Training details. Most of the hyperparameters take the same values as CAT-SAC, presented in Tab. 2. For some hyperparameters with different values, we tag them with '(toy)' in the table. The visualization results of the prediction error of RND and X-RND are presented in Fig. 5 and Fig. 6, respectively. From these figures, we can observe the X-RND can maintain the curiosity about distant states with feature input.

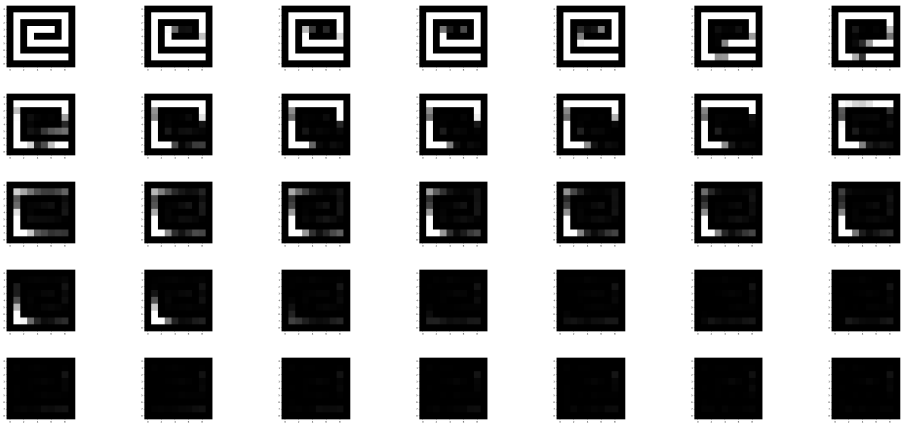

Figure 5: The prediction errors of all blocks of RND. These figures are obtained by using RND to predict the curiosity about all states after training with different numbers of visited states. From left to right and from top to bottom, the number of visited states is increasing.

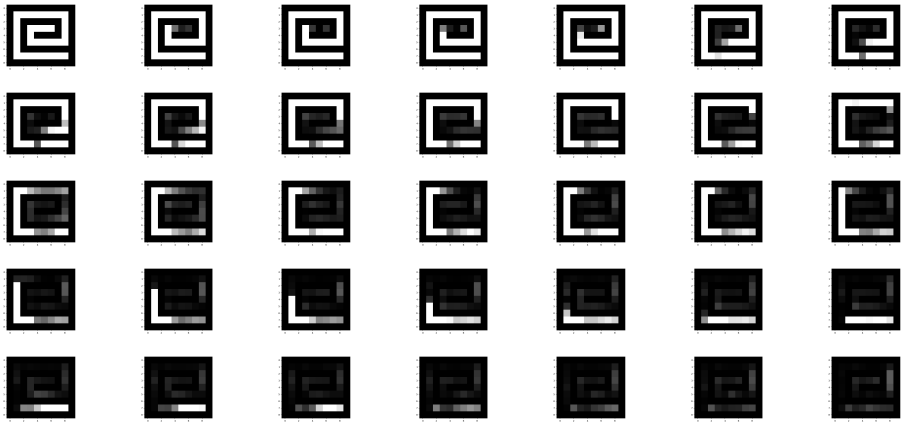

Figure 6: The prediction errors of all blocks of X-RND. These figures are obtained by using X-RND to predict the curiosity about all states after training with different numbers of visited states. From left to right and from top to bottom, the number of visited states is increasing.